Mechanistic Study of the Persistent Luminescence of CaAl2O4:Eu,Nd

ARTICLE *in* CHEMISTRY OF MATERIALS · MARCH 2015

Impact Factor: 8.54 · DOI: 10.1021/acs.chemmater.5b00288

1 AUTHOR:

Lei Wang
Hefei University of Technology
10 PUBLICATIONS **61** CITATIONS

SEE PROFILE

CHEMISTRY OF MATERIALS

Article

pubs.acs.org/cm

Mechanistic Study of the Persistent Luminescence of $CaAl_2O_4$:Eu,Nd

Bingyan Qu,[†] Bo Zhang,[†] Lei Wang,*[,†] Rulong Zhou,*[,†] and Xiao Cheng Zeng*[,‡]

[†]School of Materials Science and Engineering, Hefei University of Technology, Hefei, Anhui 230009, P. R. China

[‡]Department of Chemistry and Nebraska Center for Materials and Nanoscience, University of Nebraska—Lincoln, Lincoln, Nebraska 68588, United States

ABSTRACT: $CaAl_2O_4$:Eu is a persistent luminescence (PL) material in the blue light region with potentially wide commercial applications. With the doping of Nd, the decay time can be elongated to more than 19 h. These excellent properties are believed to be in close relation with the electronic structures of the dopants, the defects, and the host material. In this work, we attempt to achieve a better understanding of the PL mechanism of $CaAl_2O_4$:Eu based on first-principles calculations. The electronic structures of the host $CaAl_2O_4$, the luminescent center Eu, the O and Ca vacancies, and the dopant Nd are systematically studied. According to the calculations, the 4f and 5d levels of Eu are located within the band gap and slightly above the conduction band minimum (CBM), respectively. The electrons on the 4f levels can be excited into the 5d levels via ultraviolet radiation. The excited electrons on the 5d levels can move to the conduction bands and become free electron carriers. The electron carriers can be trapped for a short period by the empty defect levels below the CBM if they are very close to the defects and then return back into the conduction band. After the trap−release process, the electrons may re-enter the 5d levels of Eu and then move back to the 4f levels accompanied by light emission. The +2 charged-state O vacancies can serve as electron traps. The Ca vacancies cannot contribute to the PL property directly but can assist in stabilizing the +2 charged-state O vacancies. Nd dopants can serve as both electron donors and electron traps. These new insights into the electronic structures are useful for determining which materials may possess good PL properties, thereby motivating more experimental efforts in synthesizing improved PL materials.

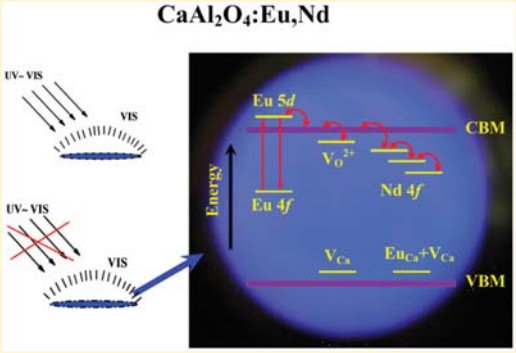

I. INTRODUCTION

$CaAl_2O_4$:Eu belongs to a class of persistent luminescence (PL) materials and possesses an excellent PL property in the blue region. It has attracted a great deal of attention because of its wide applications in energy-efficient illumination systems and infrared information displays.[1] To date, however, the PL mechanism of $CaAl_2O_4$:Eu is still being debated despite the amount of effort spent on mechanistic studies.[2−5] For this class of materials, the blue-emitting phosphors are universally viewed because of the 5d → 4f transition of Eu, while the afterglow is thought to be related to the process of capture and release of electrons between 5d levels and electron trap centers. In this view, the electron trap centers would play the key role in the PL. Another view, however, suggests that the PL of $CaAl_2O_4$:Eu stems from the hole trap centers.[6] In any case, the consensus regarding the PL mechanism has not yet been reached.[3,7]

Regardless of the type of carrier trap center, the PL mechanism is believed to be closely related to the electronic properties of the luminescent center Eu and intrinsic/extrinsic defects acting as trap centers.[4,8,9] Hence, it is important to gain deeper insights into the electronic properties of the dopants and defects, especially when they are at high concentrations.[6,9,10] For the luminescent center Eu, the 4f levels are located in the band gap while 5d levels are probably at the bottom of the conduction band.[4] With respect to the intrinsic defects, because the reducing annealing conditions and high annealing temperatures may generate both O and Ca vacancies (V_O and V_{Ca}, respectively) in $CaAl_2O_4$:Eu, the roles of these defects are expected to be crucial to the PL phenomena. In the literature, V_O is supposed to serve as an electron trap center[4] while V_{Ca} possibly acts as a hole trap center[6,11,12]. However, "solid" evidence for these assumptions is still lacking. The distribution of O and Ca vacancies and their influence on the PL property of $CaAl_2O_4$:Eu are still unclear. On the other hand, the doping of Nd in $CaAl_2O_4$:Eu was found to greatly enhance the luminescence intensity and prolong the decay time.[6,13,14] Thermoluminescence experiments showed that Nd can increase the depth of the trap of $CaAl_2O_4$:Eu in the band structure of the host material, which can be viewed as the main reason for the prolonged decay time.[15] However, the depths of these traps are difficult to measure accurately in experiments, and thus, it is hard to evaluate the influence of them on the persistent phosphors.[7,12] Dorenbos,[4] Hölsä, and many others[12,16,17] proposed that the co-doped Nd itself can act as a potential electron trap, while Matsuzawa et al.[6] reported that Nd serves as the hole trapping center based on the hole-type

Received: January 22, 2015
Revised: February 27, 2015
Published: March 3, 2015

DOI: 10.1021/acs.chemmater.5b00288
Chem. Mater. 2015, 27, 2195−2202

photoconductivity observed in $CaAl_2O_4$:Eu,Nd. To clarify these contradictory results, it is important to compute the defect levels of Nd and understand their influence on the electronic structure of $CaAl_2O_4$:Eu.

First-principles calculations can provide detailed information about the band structures of the host material $CaAl_2O_4$, energy levels of the luminescence center Eu, and defects. Here, we investigate the formation, distribution, and electronic structure of Eu, Nd, V_O, and V_{Ca} in the $CaAl_2O_4$ host to understand how these dopants and defects affect the PL of $CaAl_2O_4$:Eu. We observe that the electron-occupied 4f energy levels of Eu are located within the band gap of $CaAl_2O_4$, while the empty 5d levels are just above the conduction band minimum (CBM), suggesting that the electronic transition between 4f and 5d levels of Eu is most likely the origin of the luminescence. The +2 charged O vacancies (V_O^{2+}) act as the electron trap centers because their energy levels are located below the conduction band and close to the CBM. The Ca vacancies introduce shallow acceptor levels, which cannot directly contribute to the PL but can contribute to the stabilization of V_O^{2+}. The doped Nd not only can introduce additional electron carriers but also can serve as a deep electron trap. Therefore, the doping of Nd can significantly enhance the PL of $CaAl_2O_4$:Eu. Our calculations are in good agreement with the experimental results.

II. COMPUTATIONAL DETAILS AND MODELING

All the calculations were conducted by using the Vienna ab initio simulation package (VASP).[18,19] The projector augment wave (PAW) pseudopotentials were adopted to describe the interactions of elements, where the valence configurations of O, Al, Ca, Eu, and Nd were $2s^22p^4$, $3s^23p^1$, $3s^23p^64s^2$, $4f^75s^25p^66s^2$, and $4f^45s^25p^66s^2$, respectively. The Perdew–Burke–Ernzerof (PBE) exchange-correlation functional within the generalized gradient approximation (GGA)[19] was selected. To describe the strongly correlated 4f electrons of Eu, the GGA+U method following the formulation suggested by Dudarev et al.[20] was used. A plane-wave basis set with an energy cutoff of 400 eV was adopted. Considering the size of the cell used (see Figure 1), a $4 \times 4 \times 2$ Γ-centered k mesh was adopted for the K-point sampling. The ionic positions were fully relaxed until the residual force acting on each ion was less than 0.01 eV/Å.

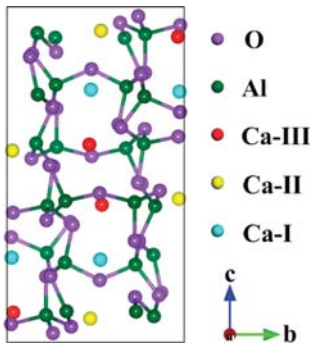

Figure 1. Unit cell of $CaAl_2O_4$. Color scheme: green for Al, violet for O, and cyan, yellow, and red are for Ca-I–Ca-III, respectively.

The crystal structure of the perfect $CaAl_2O_4$ compound is shown in Figure 1, which belongs to the monoclinic crystalline system and possesses the $P2_1/c$ space group. The optimized lattice parameters of a, b, c, and β are 8.673 Å, 8.020 Å, 15.182 Å, and 90.231°, respectively, in good agreement with the experimental results.[21,22] This structural framework was composed by vertex-sharing AlO_4 tetrahedra with Ca atoms inserted in the interstitials. On the basis of different coordination environments, the Ca atoms can be classified into three groups (denoted Ca-I, Ca-II, and Ca-III). Ca-I is coordinated with nine O atoms, while both Ca-II and Ca-III are coordinated with six O atoms. The mean distances between the Ca atoms and their nearest-neighbor O atoms are 2.824, 2.392, and 2.390 Å for Ca-I–Ca-III, respectively.

The defective structural models were obtained through substitution of one of the Ca atoms using a Eu or Nd atom (Eu_{Ca} or Nd_{Ca}), or removing one of the Ca or O atoms in one conventional cell of $CaAl_2O_4$ (whose stoichiometry is $Ca_{12}Al_{24}O_{48}$). The single defects of Eu_{Ca}, Nd_{Ca}, V_{Ca}, and V_O, as well as the complex defects Eu_{Ca}+V_{Ca}, Eu_{Ca}+Nd_{Ca}, and Eu_{Ca}+V_O, are studied in this work.

III. RESULTS AND DISCUSSION

1. Stabilities of Defects. The formation energies of defects are calculated according to the formula

$$E_F = E(Ca_{12-x}Al_{24}O_{48-y}X_z) - E(Ca_{12}Al_{24}O_{48}) - z\mu_X + x\mu_{Ca} + y\mu_O \quad (1)$$

where $E(Ca_{12}Al_{24}O_{48})$ and $E(Ca_{12-x}Al_{24}O_{48-y}X_z)$ (X = Eu or Nd) represent the total energies of the compound without and with defects, respectively, and μ_X, μ_{Ca}, and μ_O are the chemical potentials of the bulk X, Ca, and O_2 molecule, respectively. For the single defects Eu_{Ca}, Nd_{Ca}, and V_{Ca}, the calculated results are summarized in Table 1. Apparently, the defect occupying the

Table 1. Formation Energies (in electronvolts) of the Single Defects Eu_{Ca}, Nd_{Ca}, and V_{Ca}

	Ca-I	Ca-II	Ca-III
Eu_{Ca}	0.136	0.581	0.677
Nd_{Ca}	0.646	1.176	1.272
V_{Ca}	9.207	9.742	10.202

Ca-I site has the lowest formation energy, which is ∼0.45 eV lower than that at the Ca-II or Ca-III site. Such a large energy difference indicates that these defects should show strong tendencies to occupy the Ca-I site, consistent with previous experimental observation. The occupation of the Ca-I site is reasonable because the average distance between O atoms and Ca-I is much longer than that between O atoms and Ca-II or Ca-III. The longer the distance between Ca atoms and O atoms, the weaker the interaction between them. Hence, removing Ca-I is expected to be much easier than removing Ca-II or Ca-III.

It is also believed that the O vacancies play an important role in the long persistence luminescence materials.[4,13] When one O atom is removed, two unpaired electrons left can be easily ionized. So V_O in $CaAl_2O_4$ may be in charged states. To evaluate which charge state of V_O is more stable, we calculate their formation energies and study their variation with the Fermi energy, according to formula 2:[23]

$$E_F = E^q(Ca_{12}Al_{24}O_{47}) - E(Ca_{12}Al_{24}O_{48}) - \mu_O + q\varepsilon_f \quad (2)$$

where $E^q(Ca_{12}Al_{24}O_{47})$ represents the total energy of the compound containing a charged O vacancy, q is the charge of V_O, and ε_f is the Fermi level of the system. The calculated formation energies as a function of the Fermi level are shown in Figure 2. The slope of the lines in the figure corresponds to the charge state of the O vacancy. The O vacancy at neutral charge state obviously has the lowest energy when the Fermi level is higher than 1.40 eV [reference to the valence band maximum

DOI: 10.1021/acs.chemmater.5b00288
Chem. Mater. 2015, 27, 2195–2202

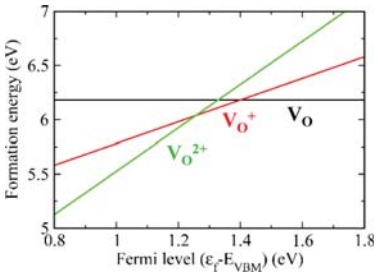

Figure 2. Calculated O vacancy formation energies at different charge states as a function of the Fermi level.

(VBM)], while V_O^{2+} becomes more stable when the Fermi level is below 1.33 eV. The V_O^{+} is stable when the Fermi level is in the range of 1.33−1.40 eV. Considering the calculated band gap of $CaAl_2O_4$, which is ∼4.54 eV (see the next section), the Fermi level at 1.33 or 1.40 eV is somewhat closer to the VBM than to the CBM. Thus, the +2 and +1 charged O vacancies are stable at the hole doping compound, while the neutral O vacancies are stable in the prefect or electron doping cases.

If Eu_{Ca} already exists, how will V_{Ca}, V_O^{2+}, or Nd_{Ca} be distributed? To answer this question, we consider the complex defects Eu_{Ca}+X, where X represents V_{Ca}, V_O^{2+}, or Nd_{Ca}. We calculated the formation energies of these complex defects when the separation distance between Eu_{Ca} and X is shortest or infinite. The results are 7.715 and 9.343 eV in the case of Eu_{Ca}+V_{Ca}, 3.944 and 3.785 eV in the case of Eu_{Ca}+V_O^{2+} (the Fermi level is set at VBM), and 0.812 and 0.783 eV in the case of Eu_{Ca}+Nd_{Ca}, respectively. Obviously, V_{Ca} and Eu_{Ca} tend to be located close to each other because the formation energy decreases remarkably when both are close, while V_O^{2+} and Nd_{Ca} tend to stay away from Eu_{Ca} because the formation energies decrease when the separation distance between them increases.

2. Electronic Structures. First, we briefly discuss the electronic structure of the perfect compound $CaAl_2O_4$. Computed band structures and the total and partial densities of states (DOS and PDOS, respectively) of perfect $CaAl_2O_4$ are shown in Figure 3. Clearly, $CaAl_2O_4$ is an insulator with a computed band gap (GGA-PBE) of 4.54 eV. Hölsä et al. reported a measured value of 6.7 eV for $CaAl_2O_4$, based on the UV−VUV synchrotron radiation excitation spectra.[24] This value is actually the optical gap rather than the electronic band gap. Considering the uncertainty of the experiment, the realistic electronic band gap is expected to be less than 6.7 eV. In ref 25, a value of 5.8 eV is reported for the $CaAl_2O_4$ ceramic. Because many interfaces, defects, and disordered domains in the ceramic exist, the measured band gap should be smaller than that of the single crystal. To the best of our knowledge, the measured band gap of crystalline $CaAl_2O_4$ has not been reported in the literature. The realistic band gap is likely between 5.8 and 6.7 eV. As such, the computed band gap at the GGA-PBE level is 1.26−2.16 eV less than the realistic one, because of the well-known limitation of GGA-PBE in predicting band gaps of semiconductors and insulators. To address this bandgap underestimation issue, one can shift the computed band gap into the experimental one by using the scissor correction method. Because density functional theory can usually predict an accurate valence band while underestimating the energies of the conduction band, here, a scissor operation of 1.26−2.16 eV is applied to the conduction band (see discussions below) so that the computed band gap would be consistent with the experimental one.

The single-crystalline structure of $CaAl_2O_4$ is mainly composed of AlO_4 tetrahedra. Therefore, the bonding orbitals of Al−O bonds contribute mainly to the valence bands. From the PDOS shown in Figure 3a, we see that the 2p states of O have the largest contribution to the valence bands while the states of Ca show little contribution. The charge density distribution of the highest-valence band (Figure 3c) also confirms the valence bands are mainly contributed by O. On the other hand, the antibonding orbitals of the Al−O bonds contribute to the low conduction bands. From the PDOS (Figure 3a) and the charge density distribution (Figure 3b), we see that the 3d orbitals of Ca and the antibonding orbitals of Al−O are the main contribution to the lowest-conduction band.

a. Eu Doping in $CaAl_2O_4$. The electronic structures of Eu-doped $CaAl_2O_4$ are computed. Here, only the substitution of Ca-I by Eu is considered as it results in the lowest formation energy. The computed band structure and PDOS of Eu_{Ca} are shown in Figure 4. Via comparison to the DOS of perfect compound $CaAl_2O_4$ (Figure 3), one can see that the doped Eu introduces impurity levels into the band gap. The PDOS indicates that the impurity levels stem from Eu 4f orbitals. The Fermi level lies above the impurity levels, suggesting that the impurity levels are occupied by electrons. The impurity bands are very flat, suggesting weak interaction between Eu ions and the host. Therefore, the scissor correction to the conduction bands of $CaAl_2O_4$ would not significantly affect the position of

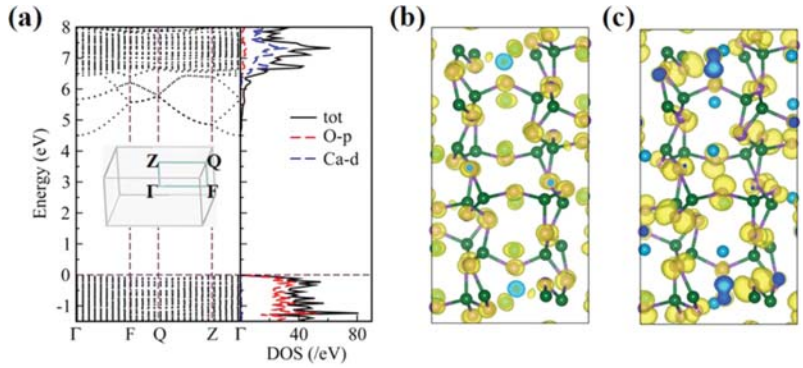

Figure 3. (a) Computed electronic band dispersion, DOS, and PDOS of the prefect compound $CaAl_2O_4$. The isosurface of the charge density of the lowest-conduction band (b) and the highest-valence band (c). The Fermi level is set to 0 eV, and the inset in panel a shows the sketch of the first Brillouin zone of $CaAl_2O_4$. In panels b and c, all Ca atoms are represented by blue spheres.

DOI: 10.1021/acs.chemmater.5b00288
Chem. Mater. 2015, 27, 2195−2202

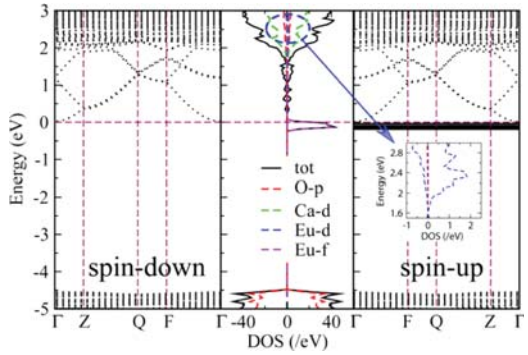

Figure 4. Computed electronic band dispersions, DOS, and PDOS of the doped compound $CaAl_2O_4$:Eu. In the band structure, all the bands are represented by the black dotted lines, except for the Eu 4f levels, which are denoted by the black solid lines. The Fermi level is set to 0 eV, and the inset in an enlarged view of Eu 5d levels.

the impurity energy levels of Eu. The empty 5d levels are located within the conduction bands of the host. With the scissor correction (1.26−2.16 eV), the electron-occupied 4f levels are 1.32−2.22 eV below the CBM, while the empty 5d levels are 1.04−0.14 eV above the CBM. The calculated energy difference between the 4f and 5d levels of Eu is ∼2.36 eV, smaller than the experimental value of ∼2.8 eV.[16] This energy difference is originated from the strong correlation of 4f electrons of Eu, which is underestimated by PBE computation. It can be remedied by introducing a Hubbard U correction. Through a careful test, a value of 1.4 eV for U, when added to the 4f states of Eu, can let the energy difference between the 4f and 5d levels of Eu match the experimental value. The U correction will not affect the position of 5d levels because it is added to only 4f states.

On the basis of the computed electronic structures of $CaAl_2O_4$:Eu, the PL mechanism of $CaAl_2O_4$:Eu can be explained below. According to the selection rule, the electrons can move between the 4f and 5d levels. Under UV light, the 4f electrons of Eu can be excited into the empty 5d levels. When the electrons in 5d levels move back into the 4f levels, blue emission will occur. Because the 5d levels are just above the CBM, the excited electrons in 5d can easily be transferred into the low-conduction bands and then move to elsewhere in the crystal. Some of these electrons may be trapped if empty defect levels exist just below the CBM. The electrons can stay for a while in the shallow trap and then be released back into the conduction bands. Once nearly free electrons in the conduction bands move to the site of Eu, they may move into the Eu 5d levels because the energy difference between the Eu 5d levels and the CBM is small. Consequently, persistent luminescence arises.

Note that in our structural model, the Eu concentration is ∼8.3%, which is much higher than that in experimental samples.[16] However, the impurity levels in the band structures (see Figure 4) are very flat, indicating almost no interaction between Eu atoms in the neighboring cells. Therefore, the role of Eu in our structural model (with a higher concentration) should resemble that in the low-concentration samples.

b. V_O in $CaAl_2O_4$. To prolong the luminescence time, there should be some empty defect levels below the conduction band minimum so that the electron carriers can be trapped. These defect levels should be shallow (close to the CBM) so that the trapped electrons in them can be released back into the conduction band through thermal activation. It was thought that V_O in $CaAl_2O_4$ plays the role of electron trap center for the formation of the PL, although supporting evidence is still lacking. To examine whether a defect can serve as the trap center, it is essential to show that the defect not only gives suitable impurity levels that can trap carriers and release carriers through thermal activation but also has a weak effect on the impurity levels of the luminescent center Eu. Toward this end, we compute the electronic structures of a single V_O with different charges in $CaAl_2O_4$. The band structures of V_O^0, V_O^+, and V_O^{2+} are shown in Figure 5. According to our calculation, there is no spin polarization for V_O^0 or V_O^{2+}, so their band structures for only the spin-up states are plotted. The impurity levels of O vacancies are represented by the black solid lines. As confirmed by the charge densities (Figure 5d), nearly all the charges are concentrated around the O vacancy. The charge densities of the O vacancy at different charge states are similar, so only the charge density of V_O^{2+} is shown in Figure 5d.

For V_O^0, the defect levels are ∼3 eV below the CBM, and these levels are occupied by electrons as they are located below the Fermi level. The electrons on the defect levels cannot be thermally excited into the conduction band because of the large energy gap. Hence, no rooms are left in the defect levels for electron trapping. For V_O^+, the spins are polarized, which results in the splitting of the defect levels. As shown in Figure 5, the defect levels of the spin-up states are located below the Fermi level, while those of spin-down states are located above the Fermi level. Thus, the spin-down defect states are unoccupied and can accept electrons. However, the electrons trapped in these empty states can hardly be released, again because of the large energy gap between the defect levels and the CBM. Therefore, V_O^+ in $CaAl_2O_4$ is also not an effective

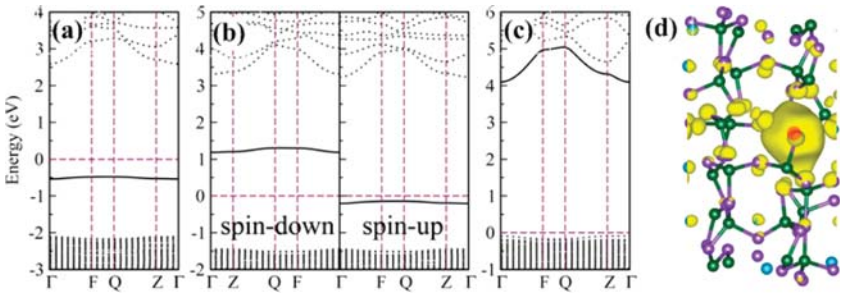

Figure 5. Computed band structures of compound $CaAl_2O_4$ with the O vacancy in (a) neutral, (b) +1, and (c) +2 charge states. (d) Computed isosurface of the charge density of the impurity level of V_O^{2+}. The impurity levels of the O vacancy are denoted by the black solid lines. The Fermi level is set to 0 eV. The O vacancy in panel d is represented by the red sphere, and all the Ca atoms are uniformly represented by the blue spheres.

DOI: 10.1021/acs.chemmater.5b00288
Chem. Mater. 2015, 27, 2195−2202

electron trap center. As for V_O^{2+}, the impurity states already have strong hybridization with the conduction band states, resulting in a nonlocalized impurity band. Because of the strong hybridization between the impurity states of V_O^{2+} and the conduction band states, the impurity band will be moved upward further if the scissor operator is applied to the conduction band. In summary, the single V_O^{2+} is an effective electron trap.

As discussed above, when V_O^{2+} approaches Eu_{Ca}, the formation energy increases, meaning that V_O^{2+} prefers being far from Eu_{Ca}. Nevertheless, we still consider the complex defect Eu_{Ca}+V_O^{2+} with the shortest distance between them to examine whether V_O^{2+} can significantly influence the electronic structures of doped Eu. The computed band structures and DOS (Figure 6) show that V_O^{2+} only slightly enlarges the

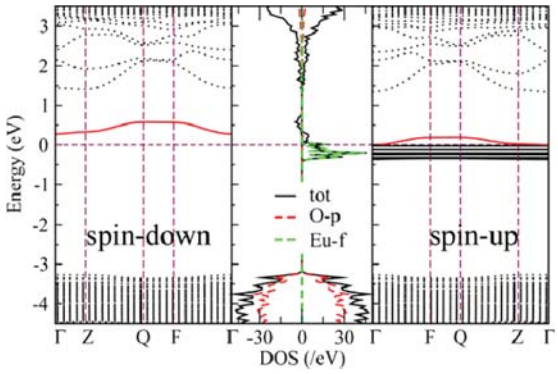

Figure 6. Computed band structure and DOS of the complex defect Eu_{Ca}+V_O^{2+} with the shortest distance between them. In the band structure, the impurity levels of the Eu 4f and O vacancy are represented by the black and red solid lines, respectively. The Fermi level is set to 0 eV.

energy gap between Eu 4f and 5d levels, implying that the influence of V_O^{2+} on the impurity levels of the luminescent center Eu and the wavelength of the luminescence is negligible. As such, V_O^{2+} can indeed serve as an electron trap center and facilitate persistent luminescence of $CaAl_2O_4$:Eu.

As mentioned above, the formation of V_O^{2+} is more favorable than that of V_O^0 and V_O^+ when the Fermi energy is below 1.33 eV (reference to the VBM). The computed band gap of perfect $CaAl_2O_4$ is ~4.54 eV. Therefore, V_O^{2+} can be stable only at the hole doping $CaAl_2O_4$. The hole-type photoconductivity observed in experiment[6] means that the O vacancy in $CaAl_2O_4$ tends to be in the +2 charge state. Hence, V_O^{2+} likely plays an important role in the persistent luminescence of $CaAl_2O_4$:Eu.

c. V_{Ca} in $CaAl_2O_4$. V_{Ca} is another intrinsic defect commonly present in the $CaAl_2O_4$ compound.[24] It was thought to be either electron or hole traps.[6,12] The electronic structure of V_{Ca} should be much different from that of V_O because in the compound Ca loses electrons while O accepts electrons. Removing one Ca atom would leave two unpaired electrons. Because the two unpaired electrons tend to be associated with O atoms, they are difficult to detach from O atoms. The unsaturated O atoms can also draw electrons from other places because of their high electronegativity. Hence, the V_{Ca} should act as a hole trap rather than an electron trap. Our calculations support this view. As shown in Figure 7, for the single V_{Ca} in $CaAl_2O_4$, there are spin-down impurity bands located above the

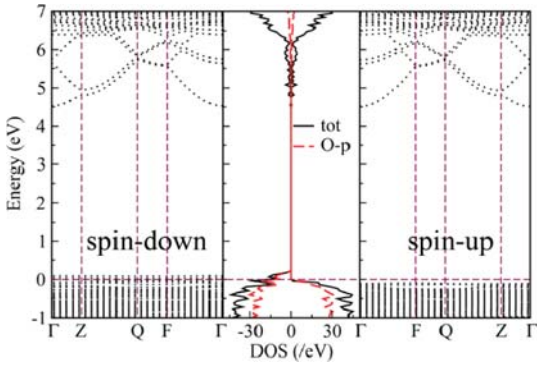

Figure 7. Computed band structure, DOS, and PDOS of $CaAl_2O_4$ with V_{Ca} occupying the Ca-I site. The transverse line represents the Fermi level.

Fermi level and very close to the valence band maximum. These empty impurity levels can accommodate electrons excited from the valence band leaving hole carriers behind. Therefore, the $CaAl_2O_4$ compound with V_{Ca} is expected to exhibit hole-type conductivity. The hole-type photoconductivity of $CaAl_2O_4$:Eu was indeed found by Matsuzawa et al. in their experiment,[6] demonstrating the existence of Ca vacancies in the system. Because the $CaAl_2O_4$ compound with Ca vacancies exhibits hole-type conductivity, the Fermi level should be close to the valence band. As discussed above, the lower the Fermi level, the smaller the formation energy of V_O^{2+}. Thus, the existence of V_{Ca} should assist the formation of V_O^{2+}, thereby prolonging the PL. In the band structures, no empty defect bands are near the CBM. Thus, V_{Ca} in $CaAl_2O_4$ is not an electron trap center.

According to the calculated formation energies, V_{Ca} favors formation near the Eu impurities in $CaAl_2O_4$:Eu, so there may be strong interaction between Eu_{Ca} and V_{Ca} if they are close. In this case, the electronic structure may be very different from that if Eu_{Ca} and V_{Ca} are far from one another. Whether V_{Ca} is beneficial or harmful to the PL properties of $CaAl_2O_4$:Eu is still an open question. To shed light on this issue, we compute the electronic structure of the complex defect Eu_{Ca}+V_{Ca} (see Figure 8). Compared to Figure 4, it can be seen that the occupied 4f levels of single defect Eu_{Ca} disappear from the band gap. Instead, empty Eu 4f levels arise and are located just above the Fermi level while the occupied Eu 4f levels move to the valence band. The Eu 5d levels are slightly affected and still located above the CBM. The energy difference between Eu 5d levels and the occupied Eu 4f levels is so large that the luminescence

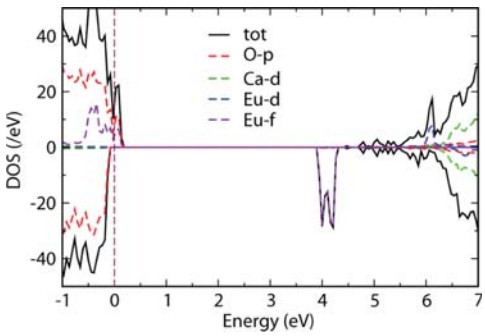

Figure 8. Computed DOS and PDOS of $CaAl_2O_4$ with V_{Ca} and Eu_{Ca}. The Fermi level is set to 0 eV.

DOI: 10.1021/acs.chemmater.5b00288
Chem. Mater. 2015, 27, 2195−2202

of the wavelength observed in the experiment should disappear in this case.

What happened for the Eu ion when a V_{Ca} formed nearby? To address this question, we compare the PDOS of Eu_{Ca} with and without V_{Ca} nearby. For the Eu_{Ca} without V_{Ca} nearby (Figure 4), the 5s and 5p levels are fully occupied as they are far below the Fermi level for both spin-up and spin-down states. For the 4f levels, those for spin-up states are below the Fermi level, while those for the spin-down states are far above the Fermi level. By counting the energy eigenvalues at each k-point, we learn that there are seven 4f bands below the Fermi level. Because the Eu atom has seven 4f electrons, the spin-up 4f bands are fully filled. The 6s levels are empty because they are above the Fermi level (>10 eV higher), meaning that the two 6s electrons of Eu are lost; i.e., Eu_{Ca} is in the +2 valence state in this case. On the other hand, for the Eu_{Ca} with V_{Ca} nearby (Figure 8), the spin-up 4f levels split. Some spin-up 4f levels move above of the Fermi level so that these levels are unoccupied. Compared to the case of Eu_{Ca} without V_{Ca}, Eu loses more 4f electrons in this case; i.e., it is in a higher-valence state. It is known that Eu^{2+} ions in $CaAl_2O_4$ give an emission broad band in the range of 410−550 nm, whereas Eu ions with a higher-valence state cannot. Our calculations are consistent with experimental observation.

In summary, low-density V_{Ca} in $CaAl_2O_4$:Eu can be beneficial to the persistent luminescence as they can lower the formation energy of V_O^{2+}, which acts as an electron trap center. High-density V_{Ca} should be harmful to the luminescence of $CaAl_2O_4$:Eu as they are highly likely to be located near Eu, which would transform the valence state of Eu ion from +2 to higher-valence states.

d. Nd Doping in $CaAl_2O_4$. Previous experiments indicate that slight doping of Nd into $CaAl_2O_4$:Eu can significantly increase the intensity and decay time of PL. However, the underlying mechanism of this doping is still unclear. Here, we compute the electronic structures of Nd-doped $CaAl_2O_4$ to investigate why and how Nd enhances persistent luminescence of $CaAl_2O_4$:Eu. As shown in Figure 9, when some Ca-I sites are substituted with Nd, spin-up impurity levels are induced near the Fermi level. From the PDOS, we see that these impurity levels originate from Nd 4f states. Some impurity levels are below the Fermi level, i.e., occupied by electrons, while others are empty. The Nd 4f levels are distributed within an energy range of ∼0.4 eV. The highest unoccupied level is approximately 0.55−1.45 eV below the CBM, with consideration of a scissor operator. The Nd 4f electrons can be excited into the conduction band by UV radiation, thereby increasing the number of electron carriers as well as the luminescence intensity. On the other hand, the empty Nd 4f levels can serve as electron traps to prolong the luminescence time. Our calculations are in good agreement with the experimental result that shows that the traps are distributed over a wide energy range of 0.5−1.2 eV.[7,10,13] Note that the depths of the Nd 4f levels are deeper than those of V_O^{2+}, so trapped electrons in Nd 4f levels are more difficult to release than those trapped in the impurity levels of V_O^{2+}. As such, the luminescence time should be prolonged significantly because of the doping of Nd.

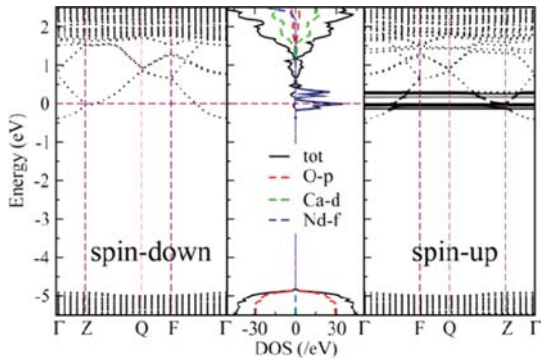

Figure 9. Computed band structure, DOS, and PDOS of the doped compound $CaAl_2O_4$:Nd with Nd occupying the Ca-I site. In the band structure, the impurity levels of Nd 4f are denoted by the black solid lines. The transverse line represents the Fermi level.

We also consider the Hubbard correction to Nd 4f states. According to the calculation, the U term renders only the occupied 4f levels moving downward but has little effect to the unoccupied 4f levels. Hence, the U term does not change the trap levels of Nd in $CaAl_2O_4$:Eu.

Next, we examine whether the co-doping of Nd in $CaAl_2O_4$:Eu changes the position of the 4f and 5d levels of Eu. As shown in Figure 10, for the Eu_{Ca}+Nd_{Ca} complex defects,

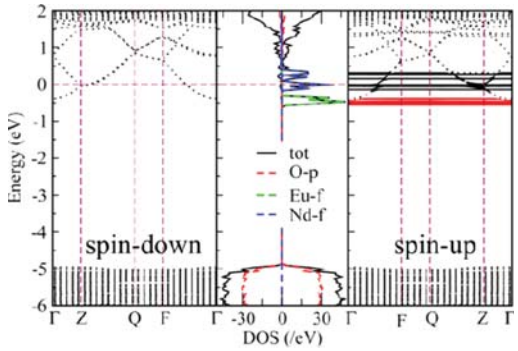

Figure 10. Computed band structure, DOS, and PDOS of the complex defects Eu_{Ca}+Nd_{Ca} with the shortest distance between them. In the band structure, the Eu 4f and Nd 4f impurity levels are represented by the red and black solid lines, respectively. The transverse line represents the Fermi level.

the impurity levels of both Eu and Nd remain unchanged as Nd atoms approach Eu, suggesting there is little interplay between levels of the two defects. Overall, the doping of Nd can indeed improve the persistent luminescence of $CaAl_2O_4$:Eu, as observed in the experiments.

3. PL Mechanism of $CaAl_2O_4$:Eu. On the basis of the analysis described above, we gain deeper insights into the PL mechanism of $CaAl_2O_4$:Eu. As illustrated in Figure 11, the excited 4f electrons of Eu can move to the empty 5d impurity levels, leaving 4f levels unoccupied. In turn, the electrons in the

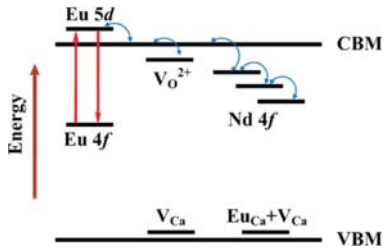

Figure 11. Schematic PL mechanism of $CaAl_2O_4$:Eu,Nd.

DOI: 10.1021/acs.chemmater.5b00288
Chem. Mater. 2015, 27, 2195−2202

5d levels can move back to 4f levels, with accompanying light emission. Moreover, the 5d electrons can also move to the conduction band, becoming free electron carriers. The electron carriers can be trapped when they encounter the O vacancy or Nd dopant. Some trapped electrons can move back to the conduction band and further move to the Eu 5d levels. As a result, they may jump back to 4f levels, leading to persistent luminescence. Typically, the doping density of Eu is very low, so that the luminescence intensity is weak without electron doping. Nd co-doping is needed to increase the luminescence intensity of $CaAl_2O_4$:Eu. The doped Nd not only can offer additional electrons but also introduce deeper electron trap centers. Consequently, Nd doping can both increase the luminescence intensity and prolong the decay time.

Why can Nd doping prolong the decay time to >19 h? First of all, the distribution of the 4f levels of Nd should play a key role. According to our calculations, Nd introduces several 4f levels into the band gap, and these levels are distributed within a medium-energy range (>0.4 eV). The lowest 4f level is quite deep (more than 1 eV below the CBM). The electron trapped in the lowest 4f level of Nd can move to only other nearby 4f levels with the assistance of thermal vibration and phonon coupling but cannot move directly to the conduction band without radiation. Therefore, the electron has to move up and down between the 4f levels of Nd for a very long time before having a chance to move back into the conduction band when it reaches the top 4f levels of Nd or other higher trap centers, e.g., V_O^{2+}. Hence, to prolong the decay time to several hours and even several days, many empty energy levels with different energies distributed from shallow to deep positions in the band gap must be available. The wider distribution of the trap center levels, the longer the decay time beyond 19 h is expected.

Having explained the PL mechanism of $CaAl_2O_4$:Eu,Nd, we can comment on generic strategies for improving PL properties through careful selection of the host and dopants. We know that the luminescence is mainly due to the electron transition from the 5d to 4f levels. Therefore, the atomic states of the luminescent-center elements should not be strongly influenced by the host; i.e., the luminescent-center elements should interact only weakly with the host. To meet this requirement, sufficient room is needed in the host to accommodate the doped luminescent-center elements without inducing large structural deformation. Indeed, $CaAl_2O_4$ belongs to this kind of host because substitution of Ca with rare-earth elements introduces little structural deformation. A reason is that the Ca ion radius (0.99 Å) is very close to those of the rare-earth elements (from 1.06 Å for La to 0.85 Å for Lu). There may be many other compounds meeting this requirement.

To maintain persistent luminescence, the excited electrons in 5d levels are required to be able to move to other places before moving back to 4f levels. Therefore, the 5d levels of the luminescent-center elements should be either above or slightly below the CBM of the host. If the 5d levels are above the CBM, they should be not too high as the electron carriers in the low-conduction band should be able to move to the 5d levels through thermal activation. Because typically the doping density of the luminescent-center elements is very small, electron doping is necessary to achieve strong luminescent intensity. Co-doping of higher-valence-state rare-earth elements is an effective way to enhance the luminescent intensity. To prolong the decay time, empty defect levels distributed over a wide energy range and being located from shallow to deep positions in the band gap are required.

IV. CONCLUSION

We have investigated the PL mechanism of $CaAl_2O_4$:Eu based on first-principles calculations. Particular attention has been paid to the electronic structures of the luminescenct-center Eu, the intrinsic vacancies of O and Ca, and the dopant of Nd. We show that the electron-occupied 4f impurity levels of Eu are located in the band gap of the host $CaAl_2O_4$, while the empty 5d impurity levels are located just above the CBM. The excited electrons in 5d impurity levels can easily transfer to the conduction band, while the electron carriers in the low-conduction band can also transfer back to the Eu 5d impurity levels easily, resulting in PL. The +2 charged-state O vacancies produce empty defect levels just below the CBM but have no significant influence on the electronic structures of Eu. Therefore, O vacancies are the main trap centers of $CaAl_2O_4$:Eu. The vacancies of Ca cannot contribute to the PL properties directly, and the high density of Ca vacancies is even harmful for the luminescence of $CaAl_2O_4$:Eu. Nevertheless, the low density of Ca vacancies can assist to stabilize the O vacancies V_O^{2+}, thereby prolonging the luminescence time. Finally, the co-doping of Nd can significantly enhance the PL properties of $CaAl_2O_4$:Eu because Nd doping not only can produce additional electron carriers but also can supply deeper electron traps. Our comprehensive study gives a detailed account of the excellent PL property of $CaAl_2O4$:Eu. Insights obtained from this study can offer some generic guiding principles for the selection of the host and the luminescent center for the design of better PL materials.

AUTHOR INFORMATION

Corresponding Authors

*E-mail: leiwang@hfut.edu.cn.
*E-mail: rlzhou@hfut.edu.cn.
*E-mail: xzeng1@unl.edu.

Notes

The authors declare no competing financial interest.

ACKNOWLEDGMENTS

This work is supported by the National Natural Science Foundation of China (Grants 11404085, 51302059, 51171055, and 11104056), the Natural Science Foundation of Anhui Province (Grant 1208085QE99), the U.S. National Science Foundation (DMR-1420645), and the University of Nebraska—Lincoln Nebraska Center for Energy Sciences Research. We thank Prof. Bicai Pan and Prof. Yuhua Wang for detailed discussion. The numerical calculations in this paper were conducted on the supercomputing system in the Supercomputing Center of the University of Science and Technology of China.

REFERENCES

(1) Thomas, M.; Daniel, S.; Cyrille, R. In *Functional Nanoparticles for Bioanalysis, Nanomedicine, and Bioelectronic Devices Volume 2*; American Chemical Society: Washington, DC, 2012; Vol. *1113*, p 1.
(2) Allix, M.; Chenu, S.; Véron, E.; Poumeyrol, T.; Kouadri-Boudjelthia, E. A.; Alahraché, S.; Porcher, F.; Massiot, D.; Fayon, F. *Chem. Mater.* **2013**, *25*, 1600.
(3) Van den Eeckhout, K.; Smet, P. F.; Poelman, D. *Materials* **2010**, *3*, 2536.
(4) Dorenbos, P. *J. Electrochem. Soc.* **2005**, *152*, H107.
(5) Hölsä, J.; Laamanen, T.; Lastusaari, M.; Malkamäki, M.; Novák, P. *J. Lumin.* **2009**, *129*, 1606.

DOI: 10.1021/acs.chemmater.5b00288
Chem. Mater. 2015, 27, 2195−2202

(6) Matsuzawa, T.; Aoki, Y.; Takeuchi, N.; Murayama, Y. *J. Electrochem. Soc.* **1996**, *143*, 2670.
(7) Van den Eeckhout, K.; Bos, A. J. J.; Poelman, D.; Smet, P. F. *Phys. Rev. B* **2013**, *87*, 11.
(8) Hölsä, J.; Aitasalo, T.; Jungner, H.; Lastusaari, M.; Niittykoski, J.; Spano, G. *J. Alloys Compd.* **2004**, *374*, 56.
(9) Jia, D.; Yen, W. M. *J. Electrochem. Soc.* **2003**, *150*, H61.
(10) Wang, L.; Chen, Y.; Zhou, R.; Xu, Y.; Wang, Y. *ECS J. Solid State Sci. Technol.* **2012**, *1*, R72.
(11) Xu, X. H.; Yu, X.; Zhou, D. C.; Qiu, J. B. *Mater. Res. Bull.* **2013**, *48*, 2390.
(12) Aitasalo, T.; Hölsä, J.; Jungner, H.; Lastusaari, M.; Niittykoski, J. *J. Phys. Chem. B* **2006**, *110*, 4589.
(13) Aitasalo, T.; Dereń, P.; Hölsä, J.; Jungner, H.; Krupa, J. C.; Lastusaari, M.; Legendziewicz, J.; Niittykoski, J.; Stręk, W. *J. Solid State Chem.* **2002**, *171*, 114.
(14) Wang, Y.; Wang, L. *J. Appl. Phys.* **2007**, *101*, 053108.
(15) Aitasalo, T.; Durygin, A.; Holsa, J.; Lastusaari, M.; Niittykoski, J.; Suchocki, A. *J. Alloys Compd.* **2004**, *380*, 4.
(16) Lin, Y. H.; Tang, Z. L.; Zhang, Z. T.; Nan, C. W. *J. Eur. Ceram. Soc.* **2003**, *23*, 175.
(17) Kumar, K.; Singh, A. K.; Rai, S. B. *Spectrochim. Acta, Part A* **2013**, *102*, 212.
(18) Kresse, G.; Hafner, J. *Phys. Rev. B* **1993**, *47*, 558.
(19) Kresse, G.; Furthmüller, J. *Phys. Rev. B* **1996**, *54*, 11169.
(20) Dudarev, S.; Botton, G.; Savrasov, S.; Humphreys, C.; Sutton, A. *Phys. Rev. B* **1998**, *57*, 1505.
(21) Dougill, M. W. *Nature* **1957**, *180*, 292.
(22) Jiang, N. *J. Appl. Phys.* **2006**, *100*, 0137031.
(23) Kohan, A.; Ceder, G.; Morgan, D.; Van de Walle, C. *Phys. Rev. B* **2000**, *61*, 15019.
(24) Hölsä, J.; Laamanen, T.; Lastusaari, M.; Malkamäki, M.; Niittykoski, J.; Novák, P. *Radiat. Phys. Chem.* **2009**, *78*, S11.
(25) Jia, D.; Wang, X.-j.; Yen, W. M. *Chem. Phys. Lett.* **2002**, *363*, 241.

DOI: 10.1021/acs.chemmater.5b00288
Chem. Mater. 2015, 27, 2195−2202